

Electrostatic-controlled parity switching in InAs-Al hybrid Coulomb island without Zeeman effect

Xiao-Fan Shi(史小凡), Guo-An Li(李国安), Dong Pan(潘东), Guang Yang(杨光), An-Qi Wang(王安琪), Zhi-Yuan Zhang(张志远), Xiao Deng(邓啸), Yu-Peng Li(李宇鹏), Zhao-Zheng Lyu(吕昭征), Pei-Ling Li(李沛岭), Fan-Ming Qu(屈凡明), Guang-Tong Liu(刘广同), Jian-Hua Zhao(赵建华), Zi-Wei Dou(窦子威), Li Lü(吕力), Jie Shen(沈洁)
Citation: Chin. Phys. B. 35, 097304 (2026). DOI: 10.1088/1674-1056/ae6f9a |
CSTR: 32038.14.CPB.ae6f9a
http://cpb.iphy.ac.cn; http://iopscience.iop.org/cpb

What follows is a list of articles you may be interested in

Modulating electronic properties of carbon nanotube via constructing one-dimensional vdW heterostructures

Wenqi Lv(吕雯祺), Weili Li(李伟立), Wei Ji(季威), Yanning Zhang(张妍宁)
Chin. Phys. B. 34, 067303 (2025). DOI: 10.1088/1674-1056/adc406 | CSTR: 32038.14.CPB.adc406

Pure spin-current diode based on interacting quantum dot tunneling junction

Zhengzhong Zhang(张正中), Min Yu(余敏), Rui Bo(薄锐), Chao Wang(王超), Hao Liu(刘昊)
Chin. Phys. B. 30, 117305 (2021). DOI: 10.1088/1674-1056/abfbd8

Transition from the Kondo effect to a Coulomb blockade in an electron shuttle

Zhang Rong(张荣), Chu Wei-Dong(楚卫东), Duan Su-Qing(段素青), Yang Ning(杨宁)
Chin. Phys. B. 22, 117305 (2013). DOI: 10.1088/1674-1056/22/11/117305

Thermoelectric transport through a quantum dot with a magnetic impurity

Yu Zhen(于震), Guo Yu(郭宇), Zheng Jun(郑军), Chi Feng(迟锋)
Chin. Phys. B. 22, 117303 (2013). DOI: 10.1088/1674-1056/22/11/117303

RAPID COMMUNICATION

Electrostatic-controlled parity switching in InAs–Al hybrid Coulomb island without Zeeman effect

Xiao-Fan Shi(史小凡)[1,2,†], Guo-An Li(李国安)[1,†], Dong Pan(潘东)[3,‡], Guang Yang(杨光)[1], An-Qi Wang(王安琪)[1], Zhi-Yuan Zhang(张志远)[1,2], Xiao Deng(邓啸)[1,2], Yu-Peng Li(李宇鹏)[4], Zhao-Zheng Lyu(吕昭征)[1], Pei-Ling Li(李沛岭)[1], Fan-Ming Qu(屈凡明)[1,2,5], Guang-Tong Liu(刘广同)[1,5], Jian-Hua Zhao(赵建华)[3,6], Zi-Wei Dou(窦子威)[1,§], Li Lü(吕力)[1,2,5,¶], and Jie Shen(沈洁)[1,2,||]

[1] *Beijing National Laboratory for Condensed Matter Physics, Institute of Physics, Chinese Academy of Sciences, Beijing* 100190, *China*
[2] *University of Chinese Academy of Sciences, Beijing* 100049, *China*
[3] *State Key Laboratory of Semiconductor Physics and Chip Technologies, Institute of Semiconductors, Chinese Academy of Sciences, Beijing* 100083, *China*
[4] *Hangzhou Key Laboratory of Quantum Matter, School of Physics, Hangzhou Normal University, Hangzhou* 311121, *China*
[5] *Hefei National Laboratory, Hefei* 230088, *China*
[6] *National Key Laboratory of Spintronics, Hangzhou International Innovation Institute, Beihang University, Hangzhou* 311115, *China*

(Received 12 May 2026; revised manuscript received 18 May 2026; accepted manuscript online 19 May 2026)

The ground-state parity in superconductor-semiconductor hybrid systems indeed plays a pivotal role in both the pursuit of Majorana zero modes (MZMs) and the development of topological qubits. Here, we report the gate control of a ground-state parity switch in an InAs–Al hybrid nanowire Coulomb island without the Zeeman effect. The evolution in Coulomb-blockaded spectroscopy reveals a gate-driven crossing of a subgap state through zero energy, revealing characteristics of a spin-polarized Andreev bound state (ABS). Our findings indicate the presence of spin splitting without a Zeeman field and demonstrate the potential for parity manipulation via purely electrostatic control and modulation.

Keywords: Majorana island, even/odd parity, nanowire hybrid device , Coulomb blockade

PACS: 73.63.–b, 73.63.Kv

DOI: 10.1088/1674-1056/ae6f9a **CSTR:** 32038.14.CPB.ae6f9a

Hybrid semiconductor–superconductor systems have attracted significant interest due to their potential for hosting Majorana zero modes (MZMs).[1–6] In these systems, a proximitized semiconductor with strong spin–orbit coupling (SOC) can undergo a topological phase transition under an external Zeeman field, leading to the emergence of zero-energy states.[7–9] However, the experimental identification of MZMs is often obscured by trivial subgap states, most notably Andreev bound states (ABSs). When these subgap states are driven to zero energy, they can produce signatures — such as zero-bias conductance peaks (ZBCPs) in tunneling spectroscopy — that are indistinguishable from those of MZMs.[10]

Coulomb-blockaded spectroscopy has been widely performed to investigate the spin and energy properties of subgap states over the last decades.[11–15] In superconducting islands, the evolution of these states is manifested through the charge periodicity of Coulomb-blockaded oscillations. When the superconducting region presents a hard gap, the oscillation of the island is 2*e* periodic corresponding to the addition of Cooper pairs. Traditionally, driving a subgap state to lower energy to trigger the oscillation transition from 2*e* to even-odd-alternating parity and then 1*e* periodicity when at zero energy, even odd-even-alternating parity when to negative energy, usually requires an external magnetic field, which lifts the spin degeneracy via the Zeeman effect.[11] In particular, 1*e* periodicity always points to the existence of an extended zero-energy state, as well as the signature of the gap closing and reopening in the island. Furthermore, to develop a Majorana-based or parity-protected qubit, the even and odd parity states can serve as robust logical states that are inherently protected against local noise.[16] Therefore, readout of the zero-energy parity is essential for implementing projective measurements and initialization of topological qubits.[17–19]

In this work, we demonstrate that the chemical potential alone can drive a subgap state across the zero-energy to the negative value[12,20] — a ground state parity switch without Zeeman field — providing new insights into the mechanism of ground-state parity switch, as well as intrinsic spin splitting and time-reversal symmetry breaking (TRSB) in these hybrid

[†]These authors contributed equally to this work.
[‡]Corresponding author. E-mail: pandong@semi.ac.cn
[§]Corresponding author. E-mail: ziweidou@iphy.ac.cn
[¶]Corresponding author. E-mail: lilu@iphy.ac.cn
[||]Corresponding author. E-mail: jieshen@iphy.ac.cn

© 2026 Chinese Physical Society and IOP Publishing Ltd. All rights, including for text and data mining, AI training, and similar technologies, are reserved.

systems. We performed Coulomb-blockaded spectroscopy on an InAs–Al hybrid nanowire island. By defining a superconducting island on the nanowire, we first observed stable Coulomb-blockaded oscillations with a $2e$ periodicity, characteristic of single Cooper pair transport. Notably, by tuning the island's chemical potential via gate voltages, we observed a switch from the initial $2e$ periodicity to an even-odd (EO) parity modulation ($S_e > S_o$), and subsequently to an odd-even (OE) parity sequence ($S_e < S_o$), all while maintaining a zero magnetic field. Here, S_e and S_o denote the oscillation peak spacings corresponding to the even and odd ground states, respectively. This reversal in the relative magnitudes of S_e and S_o provides a clear signature of the subgap state energy crossing zero-energy, signaling a parity switch in the ground state. Furthermore, our theoretical modeling demonstrates that without Zeeman field, tuning the chemical potential can effectively shift the energy levels of Andreev bound states, which allows the ABS energy to cross the zero-energy threshold, driving the ground state transition from an even parity to an odd parity ground state. The numerical simulations based on this model show a high degree of consistency with our experimental observations, accurately capturing the observed evolution of the conductance peak spacings. Whereas, the mechanism of intrinsic spin-splitting and TRSB still needs further study.

The hybrid device (Fig. 1(a)) is based on an ultra-thin InAs nanowire with a thin aluminum (Al) half shell deposited via *in-situ* molecular beam epitaxy (MBE).[21,22] The island is defined by two fine-tuned tunnel gates (TG1, TG2) that modulate the transparency of the barriers and tunnel coupling between the island and two normal-metal leads (Au). The plunger gate (PG) can be used to tune the charge number on the island, as well as the chemical potential in the hybrid region. A global backgate (BG) via the doped silicon substrate with SiO_2 layer can also modulate the chemical potential of the nanowire. A bias voltage, V_B, is applied between source (S) and drain (D). All transport measurements were performed in a dilution refrigerator at a base temperature of ~ 10 mK using standard lock-in techniques.

Figure 1(c) illustrates the differential conductance spectroscopy (dI/dV) as a function of V_{PG} and bias voltage V_B at zero field, which shows a typical $2e$ periodic Coulomb oscillation. The Coulomb diamond, outlined by the yellow dashed line, indicates the Cooper pair transport, which allows us to determine the charging energy $\sim 45\mu$eV ($e^2/2C$, for a single electron, C is the total capacitance) as detailed in supplementary Section I. Above the charge degeneracy points, the quasiparticle transport generates a blockade of Andreev reflection, resulting in negative differential conductance (NDC),[11,14] whose upper boundary aligns with induced gap Δ. Figure 1(d) shows the spectroscopy with 1T parallel magnetic field. Within the same parameter range, the oscillation period is halved, signaling the emergence of $1e$-periodic Coulomb oscillations. The transition is further elucidated by the energy level schematic in Fig. 1(e). We consider a single lowest-energy subgap state (an ABS) with energy E_0

$$E_N = E_C(N - N_G)^2 + \delta_N \times E_0, \tag{1}$$

where E_C is the Coulomb charging energy $e^2/2C$, and $N_G = C_G V_G/e$ represents the dimensionless gate-induced charge (V_G is the gate voltage, C_G is capacitance of gate). The key term δ_N captures the parity dependence of the system: $\delta_N = 1$ when N is odd, and $\delta_N = 0$ when N is even. At $B = 0$ T, the lowest-lying ABS with energy E_0 is spin-degenerate ($E_0 > E_C$, green parabola) leading the parity of ground state to be even. As $B_{ip,||}$ increases, one spin branch is lowered below E_C (represented by the blue parabola) because of the Zeeman energy corresponding to the parallel magnetic field and subsequently reaches the Fermi level (purple parabola), causing the system to transition into an odd-parity ground state. This is a quite typical transition induced by the applied magnetic field.

Since electron transport is permitted only at the cross points of the lowest-energy parabolas, the initial $2e$ periodicity oscillation first evolves into one with even-odd parity peak spacing asymmetry and then finally transitions to a uniform $1e$ periodicity oscillation once E_0 reaches zero (Fig. 1(e) bottom panel). We define the ground state spacings as $S_e = \frac{1}{\alpha}(E_C + E_0)$ and $S_o = \frac{1}{\alpha}(E_C - E_0)$, which is consistent with the extraction of individual peak spacings from Coulomb oscillations.[11,20] α is the lever arm of V_{PG}, which is extracted from the slope of Coulomb diamonds (see supplementary Section I). Then we can derive

$$\frac{E_0}{E_C} = \frac{S_e - S_o}{S_e + S_o}. \tag{2}$$

In Fig. 1(g), we can see how the oscillating peaks evolve with applied parallel magnetic field, as well as gate voltage. Because the parallel critical magnetic field is above 1 T for this thin Al,[21] the oscillating peaks at relatively high magnetic field up to 1 T (the maximum of outer magnetic field in our diluted refrigerator) are still in $1e$ superconducting regime. In particular, in Fig. 1(f), we can see obvious zero-bias conductance peaks in the diamond of Fig. 1(d), meaning the existence of an isolated zero-energy state.

Spontaneous ABSs with energy E_0 below E_C can produce even-odd parity Coulomb peak spacings without a magnetic field. However, under specific conditions, as demonstrated by Shen *et al.* (2018),[12] E_0 can cross the zero-energy threshold and reach negative values. Conventionally, such transitions are driven by an external magnetic field or the incorporation of magnetic materials,[20,23] as breaking time-reversal symmetry is typically required to lift the Kramers degeneracy

of the subgap states. In our experiment, however, we demonstrate a robust parity transition at a strictly zero magnetic field, as the following figures will show. This observation suggests that the chemical potential tuning via the plunger gate alone is sufficient to drive E_0 across zero energy, mirroring the effects typically reserved for Zeeman-field-driven regimes.

In Fig. 2(a), at zero bias, the Coulomb oscillations exhibit a stable $2e$ periodicity for gate voltages below -2.0 V, signifying an even ground-state parity. Subsequently, a splitting of the oscillation peaks emerges as E_0 drops below the charging energy, marking the onset of an even-odd ($S_e > S_o$) parity modulation. At approximately -1.28 V, the system reaches a uniform $1e$ periodicity ($S_e \approx S_o$), where E_0 reaches zero. Upon further tuning, the periodicity transitions into an odd-even parity pattern ($S_e < S_o$). This indicates that E_0 has crossed zero into negative energies, see also the case but when applying magnetic field in Shen *et al.* (2018).[12] The peak spacings, S_e and S_o, are extracted from the subtraction of the gate voltage positions (horizontal coordinates) of consecutive Coulomb peaks. According to Eq. (2), we can obtain the ratio E_0/E_C, marked by the green dotted line, which confirms that the subgap state has been lowered into the negative energy regime. The 2D mapping in Fig. 2(b) shows a clear alternating pattern of large and small Coulomb diamond regions, and a distinct parity switch is captured between -1.3 V and -1.2 V, where the charge periodicity switches. The parity switch at other gate voltages is shown in supplementary Fig. S2.

To further validate these observations, we performed Coulomb-blockaded spectroscopy on device 2 (see supplementary Fig. S3a for SEM image) in Figs. 2(c) and 2(d). The spectroscopy reveals a prominent NDC in the diamond in Fig. 2(d), the upper boundary of which aligns with the induced superconducting gap Δ, so it is always $2e$-periodic.[11] A ground-state parity switch, consistent with the behavior of device 1, can also be identified clearly through the Coulomb peak pattern, where the condition $S_e \approx S_o$ at around $V_{PG} = 1.36$ V marks the parity switch point in Fig. 2(c). Furthermore, the Coulomb diamonds associated with even-parity and odd-parity periods exhibit distinct energy scales — a characteristic asymmetry previously observed in superconducting hybrid islands. This asymmetry of energy scale between diamonds of even parity and odd parity signifies the presence of a spin-polarized ABS,[20,24] in particular without Zeeman effect at zero-field in our case. A detailed explanation will be provided later.

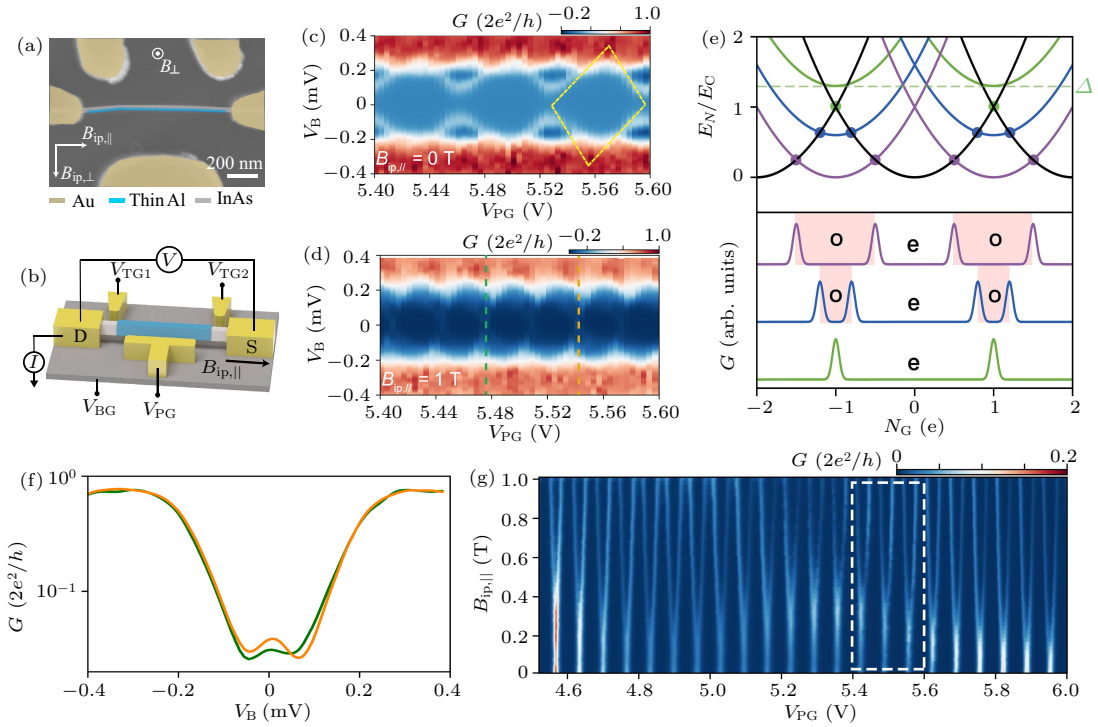


Fig. 1. Device configuration and Coulomb-blockaded characterization of the InAs–Al hybrid island. (a) False-color scanning electron micrograph (SEM) of a typical InAs–Al nanowire island device. (b) Schematic of the setup. (c) Coulomb diamonds showing differential conductance G as a function of V_B and V_{PG} without Zeeman field ($B_{ip,\parallel} = 0$ T). The upper bound of NDC represents the induced gap $\Delta \sim 220$ μeV. The charging energy $E_C \sim 45$ μeV is extracted from the Coulomb diamond. (d) Coulomb diamonds under an applied parallel magnetic field ($B_{ip,\parallel} = 1$ T, bottom). (e) Top panel: Schematic of the energy parabolas E_N for even (black) and odd (green,blue,purple) parity as a function of induced gate charge N_G. The $2e$ periodic diamond suggests the E_0 ($E_0 = \Delta$) is above E_C without the magnetic field (green parabola). Zeeman splitting drives the lowest subgap state approaching the Fermi level. Bottom panel: Corresponding Coulomb-blockaded peak traces, illustrating the evolution from $2e$ to $1e$ periodicity. The odd-state regions are highlighted in red background shading. The same coloring applies to subsequent figures. "e" means even-parity and "o" means odd-parity here. (f) Vertical linecuts taken at two charge degeneracy points in (d) showing zero-bias conductance peaks. (g) Differential conductance G plotted as a function of V_{PG} and in-plane parallel magnetic field $B_{ip,\parallel}$, displaying the evolution of Coulomb oscillations with magnetic field. The white dashed box indicates the same gate voltage range as the Coulomb diamond shown in panels (c) and (d).

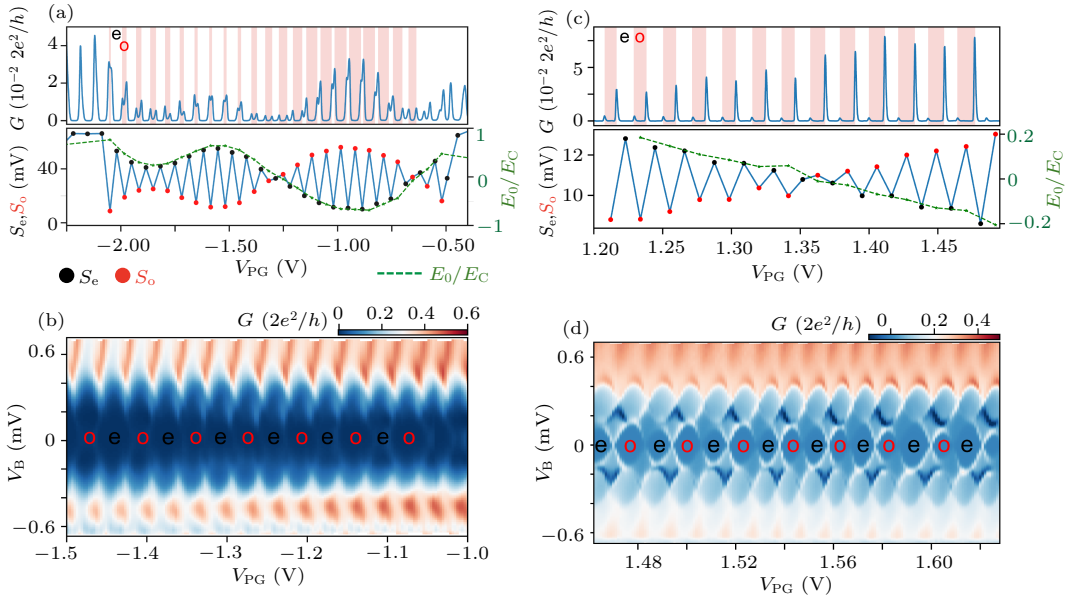


Fig. 2. Observation of gate-induced parity switch without Zeeman field. (a) Top panel: Conductance G as a function of plunger gate voltage V_{PG} for device 1 at $B = 0$ T, $V_{BG} = 5.9$ V. The periodic Coulomb peaks spaces exhibit a clear transition around -1.28 V. Bottom panel: Extracted peak spacings and the corresponding subgap state energy E_0 derived from the spacing asymmetry. The oscillation pattern shifts from even-odd parity to odd-even parity, passing through a spacing degeneracy point where $S_e \approx S_o$ ($V_{PG} \sim -1.28$ V), indicating E_0 crosses zero energy. (b) High-resolution 2D map (V_B vs. V_{PG}) of the transition region. The evolution of the shape of Coulomb diamond reflects the ground state parity switch from even to odd. (c), (d) Similar measurements for device 2, demonstrating the reproducibility of the zero-field parity switch. The spacing analysis shows a characteristic sawtooth-like evolution of the addition energy, consistent with a gate-tunable ABS.

We fabricated a third device (device 3, see SEM image in supplementary Fig. S3b) and observed a similar ground-state parity switch, as demonstrated in supplementary Fig. S4. Charge stability diagrams as a function of V_{PG} versus $V_{TG1/2}$ (supplementary Fig. S5) reveal crosstalk among the gates. Consequently, the ground-state parity can also be tuned via the tunnel gates (supplementary Fig. S6).

The observed spin polarization in zero field may be attributed to residual magnetic fields or magnetic impurities.[25] To verify the intrinsic nature of the observed zero-field parity switch, we performed systematic magnetic field sweeps in both negative-to-positive and positive-to-negative directions in Fig. 3.[23]

The device exhibited a characteristic evolution with $B_{ip,||}$ that was entirely independent of the sweep history. Without a Zeeman field — consistent with our primary observations — the parity switch persisted within the established gate voltage range, marked on Fig. 3(a). As the magnetic field strength increased by sweeping up, the subgap state energy E_0 continued its monotonic downward shift, driving the system deeper into the negative-energy regime.

Correspondingly, the conductance structure is essentially symmetric about zero magnetic field in both sweep directions. The conductance peak evolution with $B_{ip,||}$ remains the same whether the field is swept from negative to positive in Fig. 3(a) or vice versa in Fig. 3(b). These exclude the presence of any measurable residual magnetic fields. The absence of any observable hysteresis or horizontal shift in the peak positions rules out the involvement of magnetic impurities. Furthermore, it validates that the parity switch observed without Zeeman field is an intrinsic feature of our hybrid system. The same features are also confirmed in another two orthogonal directions verification, which are in-plane perpendicular $B_{ip,\perp}$ and out-of-plane $B_\perp$, as shown in supplementary Fig. S7.

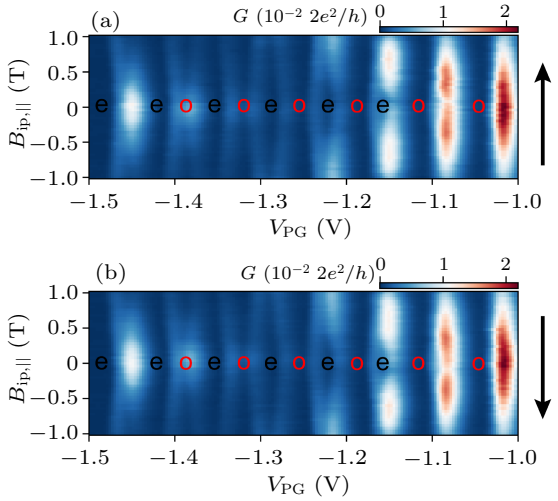


Fig. 3. Verification of zero remanent magnetic field via hysteresis scans. (a) Evolution of Coulomb peak positions as the parallel magnetic field $B_{ip,||}$ is swept from -1 T to $+1$ T (up-sweep). (b) Corresponding evolution during a down-sweep from $+1$ T to -1 T . The sweep directions are marked by the black arrow. The two datasets overlap precisely without any observable horizontal offset.

We further modeled the gate-induced parity switch using the fundamental energy-parabola framework for a superconducting nanowire island. The simulation results demonstrate qualitative agreement with the experimental data, accurately reproducing the evolution of the Coulomb oscillation peaks

during ground-state transport, as shown in Fig. 4. First, assuming that the gate-induced modulation of the chemical potential is approximately linear over a small gate range, and that the downward shift of the subgap state energy is proportional to the change in chemical potential, thus, E_0 in the Hamiltonian becomes a variable dependent on N_G. We found that within this straightforward model, increasing N_G causes E_0 to cross zero and reach negative values, resulting in a change in oscillation periodicity ($S_e > S_o$ to $S_e < S_o$) that aligns well with the experimentally observed parity switch. While the modulation of the chemical potential and energy by the gate is not always perfectly linear — explaining why the peak spacings in Fig. 2 do not exhibit ideal linearity — this simulation still achieves a high degree of consistency with the parity switch observed over small gate intervals.

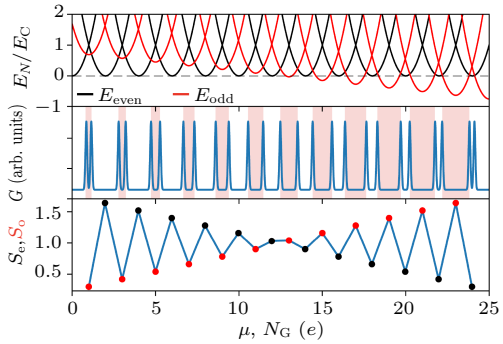


Fig. 4. Theoretical simulation of the gate-induced parity switch. Top panel: Calculated ground-state energy parabolas as a function of the chemical potential μ (or charge number N_G). Black and red curves represent even and odd parity states, respectively. The evolution of E_0 shifts the relative offset of the parabolas. A ground state parity switch occurs when the ABS crosses the Fermi level ($E_0 = 0$), where the odd-state parabola becomes the global ground state. Middle panel: Coulomb-blockaded peak positions derived from the energy parabolas. Bottom panel: The peak spacing evolves from even-odd parity (EO) periodicity to odd-even parity (OE) periodicity as E_0 approaches and crosses zero, replicating the experimental observations in Fig. 2.

Building on prior research,[20] spin-polarized ABSs in EuS-nanowire systems were identified by correlating experimental results with theoretical models. Experimentally, this is manifested as a distinct size asymmetry between Coulomb diamonds corresponding to even and odd parity. On the energy scale, these features align with the positions of $\Delta + E_0$ and $\Delta - E_0$,[20] providing strong evidence for the emergence of spin-polarized ABSs.

Consistent with this prior finding, our data reveal a pronounced size disparity between even-parity and odd-parity Coulomb diamonds, supporting the emergence of spin-polarized ABSs in our system. Crucially, while previous reports on EuS nanowires rely on the Zeeman effect to induce this polarization, our observations demonstrate that these spin-polarized features persist at zero magnetic field. Because, given the large g-factor of the InAs–Al system (~ 10), any Zeeman-induced spin polarization would inevitably manifest as a discernible zero-field offset or hysteretic splitting in bidirectional scans. However, Fig. 3 shows no such evidence; the conductance traces remain perfectly symmetric around zero field and are independent of the sweep direction. Consequently, it can be determined that the system exhibits intrinsic spin polarization in the absence of the Zeeman field, thereby ruling out the Zeeman effect as the primary mechanism.

It has been reported that in superconductor–quantum dot (SC–QD) coupled systems, a proximitized quantum dot can host Andreev bound states (ABSs) whose energy can be tuned via the chemical potential. Under specific coupling conditions, these ABSs can acquire negative energy at zero magnetic field,[26–28] leading to a singlet–doublet transition. In semiconductor–superconductor hybrid devices, the formation of an end dot between the superconducting island and the lead is a very common phenomenon. Although large–bias Coulomb blockade spectroscopy (supplementary Fig. S8) exhibits relatively regular oscillations, the measurement resolution may be insufficient to completely rule out the presence of an end-dot. Therefore, in our device, it is possible that the coupling between the end-dot and the superconductor gives rise to a singlet–doublet transition at zero magnetic field, which in turn causes the observed parity switching.

Furthermore, a multi-band effect[29–33] likely occurs in our system, where transport involves multiple hybridized subbands within the 1D channel. A plausible scenario is that the Rashba spin–orbit coupling initially splits the dispersion. Subsequently, the two lowest transport-active subbands further hybridize with each other.[32,34] But still, a source of TRSB needs to be involved. A plausible reason is that a parallel circuit exists between the half-shell Al film and the proximitized nanowire. In this scenario, a magnetic field fluctuation (approximately on the order of 10^{-3} T to 10^{-2} T, the size of the loop is 1 μm × 40 nm) could induce a subtle phase bias, thereby lifting the degeneracy of the ABSs.[35,36] But such a value of magnetic field should be distinguishable from our measurement. Therefore, the core for TRSB is still unknown. A mixture of s-wave and p-wave superconducting states might need to be considered here.[37,38]

In conclusion, in an InAs–Al hybrid Coulomb island, we observed a parity switch without a Zeeman field, characterized by the evolution of Coulomb oscillation patterns from a $2e$ periodicity to an even-odd parity (EO) pattern, and finally crossing a $1e$ periodicity to an odd-even parity (OE) sequence. This progression indicates that the energy of a subgap state (E_0) can be tuned across the zero-energy threshold to a negative value by adjusting the chemical potential via the plunger gate without a Zeeman effect. Our experimental observations, supported by energy parabola modeling and the absence of magnetic hysteresis, demonstrate that this transition is driven by electrostatic tuning rather than external magnetic effects and magnetic impurities. While the observed energy scale asymmetry suggests a potential role for ABS spin polarization, the underlying mechanism for the zero-field TRSB

remains an area for further study. This work provides an experimental demonstration of controlling ground parity through purely electrostatic means, offering insights into the behavior of subgap states in hybrid superconductor-semiconductor systems and the further parity readout for new qubits.

Acknowledgements

The works of J.S. were supported by the Beijing Natural Science Foundation (Grant No. JQ23022), the National Key Research and Development Program of China (Grant No. 2023YFA1607400). The work of Z.D. and J.S. was supported by the Young Scientists Fund of the National Natural Science Foundation of China (Grant No. 2024YFA1613200). The work of Z.D. was supported by the Strategic Priority Research Program (B) of the Chinese Academy of Sciences (CAS) (Grant No. XDB1720000) and the National Natural Science Foundation of China (Young Scientists Fund (C)) (Grant No. 12504561). The work of D.P. and J.Z. was supported by the National Natural Science Foundation of China (Grant Nos. 12374459, 61974138, and 92065106) and the Innovation Program for Quantum Science and Technology (Grant No. 2021ZD0302400). D. P. acknowledges the support from Youth Innovation Promotion Association, Chinese Academy of Sciences (Grant Nos. 2017156 and Y2021043). The works of J.S., L.L., F.Q. and G.L. were supported by the Strategic Priority Research Program B of Chinese Academy of Sciences (Grant No. XDB33000000), the National Natural Science Foundation of China (Grant Nos. 12174430 and 92365302), and the Synergetic Extreme Condition User Facility (SECUF, https://cstr.cn/31123.02.SECUF). Y.L. acknowledges support from the National Natural Science Foundation of China (Grant No. 12404154). The work of other authors was supported by the National Key Research and Development Program of China (Grant Nos. 2019YFA0308000, 2022YFA1403800, 2023YFA1406500, and 2024YFA1408400), the National Natural Science Foundation of China (Grant Nos. 12274436 and 12274459), the Beijing Natural Science Foundation (Grant No. Z200005), and the Synergetic Extreme Condition User Facility. The work is also funded by Chinese Academy of Sciences President's International Fellowship Initiative (Grant No. 2024PG0003).

References

[1] Kitaev A Y 2001 *Phys. Usp.* **44** 131
[2] Stanescu T D, Lutchyn R M and Das Sarma S 2011 *Phys. Rev. B* **84** 144522
[3] Nayak C, Simon S H, Stern A, Freedman M and Das Sarma S 2008 *Rev. Mod. Phys.* **80** 1083
[4] Plugge S, Rasmussen A, Egger R and Flensberg K 2017 *New J. Phys.* **19** 012001
[5] Aasen D, Hell M, Mishmash R V, Higginbotham A, Danon J, Leijnse M, Jespersen T S, Folk J A, Marcus C M, Flensberg K and Alicea J 2016 *Phys. Rev. X* **6** 031016
[6] Hell M, Leijnse M and Flensberg K 2017 *Phys. Rev. Lett.* **118** 107701
[7] Mourik V, Zuo K, Frolov S M, Plissard S R, Bakkers E P A M and Kouwenhoven L P 2012 *Science* **336** 1003
[8] Deng M T, Vaitiekėnas S, Hansen E B, Danon J, Leijnse M, Flensberg K, Nygård J, Krogstrup P and Marcus C M 2016 *Science* **354** 1557
[9] Microsoft Quantum 2023 *Phys. Rev. B* **107** 245423
[10] Prada E, San-Jose P, Moor M W A, Geresdi A, Lee E J H, Klinovaja J, Loss D, Nygård J, Aguado R and Kouwenhoven L P 2020 *Nat. Rev. Phys.* **2** 575
[11] Albrecht S M, Higginbotham A P, Madsen M, Kuemmeth F, Jespersen T S, Nygård J, Krogstrup P and Marcus C M 2016 *Nature* **531** 206
[12] Shen J, Heedt S, Borsoi F, Van Heck B, Gazibegovic S, Op Het Veld R L M, Car D, Logan J A, Pendharkar M, Ramakers S J J, Wang G, Xu D, Bouman D, Geresdi A, Palmstrøm C J, Bakkers E P A M and Kouwenhoven L P 2018 *Nat. Commun.* **9** 4801
[13] Hansen E B, Danon J and Flensberg K 2018 *Phys. Rev. B* **97** 041411
[14] Hekking F W J, Glazman L I, Matveev K A and Shekhter R I 1993 *Phys. Rev. Lett.* **70** 4138
[15] Valentini M, Borovkov M, Prada E, Martí-Sánchez S, Botifoll M, Hofmann A, Arbiol J, Aguado R, San-Jose P and Katsaros G 2022 *Nature* **612** 442
[16] Oreg Y, Refael G and Von Oppen F 2010 *Phys. Rev. Lett.* **105** 177002
[17] Wang J Y, Schrade C, Levajac V, Van Driel D, Li K, Gazibegovic S, Badawy G, Op Het Veld R L M, Lee J S, Pendharkar M, Dempsey C P, Palmstrøm C J, Bakkers E P A M, Fu L, Kouwenhoven L P and Shen J 2022 *Sci. Adv.* **8** eabm9896
[18] Microsoft Azure Quantum 2025 *Nature* **638** 651
[19] Van Loo N, Zatelli F, Steffensen G O, Roovers B, Wang G, Van Caekenberghe T, Bordin A, Van Driel D, Zhang Y, Huisman W D, Badawy G, Bakkers E P A M, Mazur G P, Aguado R and Kouwenhoven L P 2026 *Nature* **650** 334
[20] Vaitiekėnas S, Souto R S, Liu Y, Krogstrup P, Flensberg K, Leijnse M and Marcus C M 2022 *Phys. Rev. B* **105** L041304
[21] Pan D, Song H, Zhang S, Liu L, Wen L, Liao D, Zhuo R, Wang Z, Zhang Z, Yang S, Ying J, Miao W, Shang R, Zhang H and Zhao J 2022 *Chin. Phys. Lett.* **39** 058101
[22] Wang Z, Song H, Pan D, Zhang Z, Miao W, Li R, Cao Z, Zhang G, Liu L, Wen L, Zhuo R, Liu D E, He K, Shang R, Zhao J and Zhang H 2022 *Phys. Rev. Lett.* **129** 167702
[23] Vaitiekėnas S, Liu Y, Krogstrup P and Marcus C M 2021 *Nat. Phys.* **17** 43
[24] Higginbotham A P, Albrecht S M, Kiršanskas G, Chang W, Kuemmeth F, Krogstrup P, Jespersen T S, Nygård J, Flensberg K and Marcus C M 2015 *Nat. Phys.* **11** 1017
[25] Strambini E, Iorio A, Durante O, Citro R, Sanz-Fernández C, Guarcello C, Tokatly I V, Braggio A, Rocci M, Ligato N, Zannier V, Sorba L, Bergeret F S and Giazotto F 2020 *Nat. Nanotechnol.* **15** 656
[26] Pillet J D, Quay C H L, Morfin P, Bena C, Yeyati A L and Joyez P 2010 *Nat. Phys.* **6** 965
[27] Lee E J H, Jiang X, Houzet M, Aguado R, Lieber C M and De Franceschi S 2014 *Nat. Nanotechnol.* **9** 79
[28] Gramich J, Baumgartner A and Schönenberger C 2017 *Phys. Rev. B* **96** 195418
[29] Trimble C J, Wei M T, Yuan N F Q, Kalantre S S, Liu P, Han H J, Han M G, Zhu Y, Cha J J, Fu L and Williams J R 2021 *npj Quantum Mater.* **6** 61
[30] Yerin Y and Omelyanchouk A N 2017 *Low Temp. Phys.* **43** 1013
[31] Moroz A V 1999 *Phys. Rev. B* **60** 14272
[32] Murani A, Chepelianskii A, Guéron S and Bouchiat H 2017 *Phys. Rev. B* **96** 165415
[33] Ng T K and Nagaosa N 2009 *Europhys. Lett.* **87** 17003
[34] Governale M 2002 *Phys. Rev. B* **66** 073311
[35] Tosi L, Metzger C, Goffman M F, Urbina C, Pothier H, Park S, Yeyati A L, Nygård J and Krogstrup P 2019 *Phys. Rev. X* **9** 011010
[36] Nichele F, Portolés E, Fornieri A, Whiticar A M, Drachmann A C C, Gronin S, Wang T, Gardner G C, Thomas C, Hatke A T, Manfra M J and Marcus C M 2020 *Phys. Rev. Lett.* **124** 226801
[37] Wang Y and Fu L 2017 *Phys. Rev. Lett.* **119** 187003
[38] Wu C and Hirsch J E 2010 *Phys. Rev. B* **81** 020508